Biomaterials Science

Accepted Manuscript

This article can be cited before page numbers have been issued, to do this please use: F. Ozdemir Steedman, A. M. Ferreira-Duarte, P. Melo and K. Dalgarno, *Biomater. Sci.*, 2026, DOI: 10.1039/D6BM00467A.

ROYAL SOCIETY OF CHEMISTRY

rsc.li/biomaterials-science

View Article Online
DOI: 10.1039/D6BM00467A

ARTICLE

Bioprinting Chondrocyte Hydrogel Cultures onto Fibre Membranes for Cartilage Defect Repair

Received 00th January 20xx,
Accepted 00th January 20xx

DOI: 10.1039/x0xx00000x

Fatma Ozdemir Steedman, Ana Marina Ferreira, Priscila Melo and Kenneth Dalgarno*

* Corresponding Author, kenny.dalgarno@newcastle.ac.uk

Despite notable advancements in autologous chondrocyte implantation (ACI) over the past three decades, persistent challenges including uneven cell distribution, low seeding density, and limited extracellular matrix formation continue to hinder outcomes. This study suggests a novel approach to matrix-assisted ACI (MACI) that integrates reactive jet impingement (ReJI) bioprinting with Chondro-Gide® (Ch-G) membranes to give an in theatre bioprinting approach with the potential to control cell distribution and density at the point of implantation. A collagen–alginate–fibrin (CAF) hydrogel was formulated as a bioink to maintain high cell viability and enable accurate deposition of chondrocytes at both low and high densities. Bone marrow-derived immortalised stem cells were differentiated into chondrocytes and bioprinted using the ReJI system onto Ch-G substrates. Constructs were evaluated over 14 days for cytotoxicity, morphology, gene expression, extracellular matrix (ECM) deposition, and mechanical properties. Live/dead assays confirmed high cell viability across all conditions. Immunofluorescence and scanning electron microscope (SEM) analyses showed enhanced cell alignment, surface migration, and ECM formation, particularly in high-density Chondro-Gide®/CAF samples (Ch-G/CAF). ACAN and SOX9 showed significant upregulation from day 1 to day 14 and immunohistochemical analysis confirmed robust deposition of collagen II and sulphated glycosaminoglycans (sGAGs). Mechanical testing demonstrated increased compressive modulus over time, with Ch-G/CAF constructs exhibiting superior stiffness and volumetric stability. These findings suggest that ReJI bioprinting of CAF hydrogels onto Chondro-Gide® membranes supports enhanced chondrogenic activity and matrix formation, offering a promising strategy for next-generation MACI.

Keywords: *Bioprinting, cartilage regeneration, ACI treatment, Chondro-Gide®, hydrogel-fibre composites*

1. Introduction

Approximately 7.6% people worldwide are affected by osteoarthritis (OA) and this is predicted to increase by up to 100% by 2050 [1]. The main cause of pain in OA is damaged articular cartilage at the joint surface [2]. Articular cartilage is a smooth tissue which covers the ends of bones in a joint, consisting of water, proteoglycans, type II collagen and chondrocytes, which when healthy acts a load bearing, shock absorbing interface and provides near frictionless movement between the joint surfaces. OA causes cartilage to break down, becoming thin and damaged, and in some cases wearing away to leave exposed sub-chondral bone, causing severe pain, with the resulting effects on mobility leading to significant morbidity [3]. Articular cartilage is avascular and so has a very limited self-repair ability when damaged.

Autologous chondrocyte implantation (ACI) has been a treatment technique for articular cartilage for over 30 years but has also been continuously under development for more efficient clinical application or better treatment outcome [4]. In a first generation ACI procedure, healthy cartilage is harvested from the tibia, then chondrocytes are isolated from this and expanded ex vivo. In a second operation damaged cartilage is removed from the defect site and a harvested periosteal patch used to cover the defect site, with the expanded chondrocyte population subsequently injected under the periosteal patch to stimulate the production of new cartilage at the defect site. However, the use of the periosteum was not considered optimal, and for second generation ACI [4, 5] biomaterial scaffolds were used to encapsulate the defect volume. One of the most successful scaffolds to be used in this way is Chondro-Gide®, a fibrous collagen membrane, and this approach remains in clinical use today. Further developments in technique have led to matrix assisted autologous implantation (MACI) [6], where chondrocytes are combined with a hydrogel matrix prior to implantation to the defect site, and to the Spherox process [7], where chondrocytes are assembled into spheroids before implantation. Both MACI and the Spherox process seek to

[a] School of Engineering, Newcastle University, Newcastle upon Tyne NE1 7RU, UK.

create organised "3D" cell cultures rather than injecting cells in solution.

Low seeding cell density, cell loss during implantation and uneven distribution at the defect site are recognised limitations that can compromise the efficacy of ACI procedures [8, 9]. Interestingly, lower cell densities in ACI may lead to improved outcomes [10], although clearly there must be a lower limit to this and perhaps an optimum range. In contrast, MACI demonstrates reduced matrix deposition when seeded with low cell densities [11]. Increasing the cells per unit area or volume across a range of ACI approaches has been shown to enhance cell-cell and cell-matrix interactions, thereby enhancing more effective cartilage regeneration [12].

In the development of 3D cell cultures for tissue engineering applications bioprinting has emerged as a promising set of techniques. 3D tissue cultures can be created that closely mimic natural tissue in terms of mechanical properties, architectural design, and physiological function, with precise control over resolution and structure. In this way, cell distribution can be homogenised, and the density of cells can be increased to "optimal" number per area. The most common approach to printing hydrogel 3D cell cultures is extrusion bioprinting [13, 14] but this technique is limited in terms of (i) the ability to produce high cell densities in hydrogels [15], and (ii) the substrates that can be printed on. The Reactive Jet Impingement (ReJI) process [16] overcomes these limitations, allowing cell-filled-gels to be produced with a wide range of cell densities[17]
, from relatively low to near physiological, and with the ability to print on a wide range of hard and soft substrates in creating models [18]. Figure 1 illustrates the process, which is a quick and flexible way to create cell filled hydrogels.

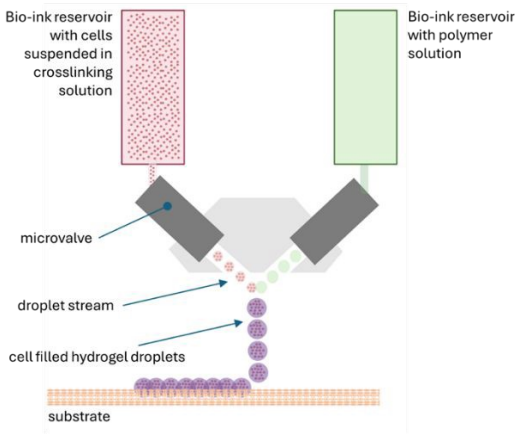

Figure 1 – Schematic of ReJI Printing Process. Microvalves are used to create droplet streams of a hydrogel pre-cursor polymer solution and a crosslinker solution. The droplets meet in mid-air and react to form a hydrogel droplet which then falls to the substrate. If cells are suspended in the polymer solution or the cross-linker solution or both then these cells will be encapsulated in the hydrogel droplet.

Here, we report an in vitro study of a new approach to MACI, which would use hydrogel encapsulated 3D bioprinted cell cultures to ensure even distribution of cells. The approach is illustrated in Figure 2 and would utilise in theatre bioprinting as a method of preparing a cell/hydrogel/fibre membrane structure for implantation. ReJI bioprinting has previously been shown to be able to produce cell-hydrogel-fibre composite structures with excellent integration and biofunctionality across a range of cell densities[18]. A collagen-alginate-fibrin (CAF) hydrogel was chosen as the bioink, as this system has previously been shown to support ReJI bioprinting of a wide range of cells and cell densities with excellent cell viability [16, 18, 19] including printing of chondrocytes [20]. To assess the effectiveness of the approach we have used matrix production as the key outcome measure and have compared cultures generated with and without Chondro-Gide®, with both high and low cell densities within the hydrogels. We evaluate cytotoxicity, morphology, proliferation, gene expression, ECM deposition and mechanical properties, with results showing that a bioprinted MACI patch has the potential to enhance cartilage tissue repair processes.

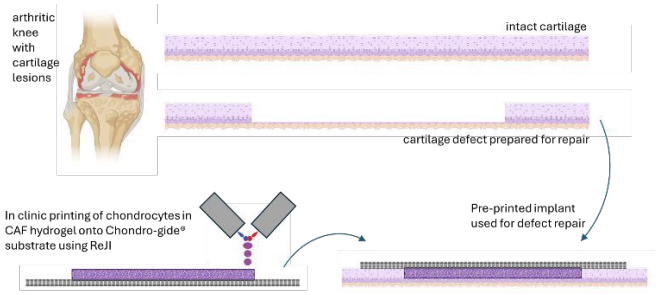

Figure 2 – Proposed Adaptation of MACI Process Using ReJI Printing. ReJI bioprinting combines a chondrocyte-filled-hydrogel with a Chrondro-gide® membrane, and the hydrogel/Chondro-Gide® construct then implanted into a prepared cartilage defect site to begin the repair process.

2. Materials and Methodology

2.1 Cell Culture

Y201 immortalised human bone marrow-derived stem cells (BMSC-hTERT) are an established stem cell line [21] with a demonstrated capacity to be differentiated into chondrocyte. Y201 derived chondrocytes (Y201-C) have been previously shown to provide an effective model cell line for the in vitro evaluation of treatments in the joint [22, 23]. Y201s were expanded in Dulbecco's Modified Eagle Medium (DMEM) with low glucose, supplemented with 10% foetal bovine serum (FBS) and 1% penicillin/streptomycin (P/S). To induce chondrogenic differentiation, Y201 cells were cultured for 21 days in serum-free DMEM supplemented with 1% P/S, 1% Insulin-Transferrin-Selenium (ITS)+1, 10 ng/mL transforming growth factor beta-3 (TGFβ-3), 40 µg/mL L-proline, 100 nM dexamethasone, and 50 µg/mL L-ascorbic acid-2-phosphate [22, 23].

Following differentiation, Y201-Cs were maintained in DMEM/F12 with high glucose (4.5 g/L), supplemented with 10% FBS, 2 mM L-glutamine, and 1% P/S. Both Y201 and Y201-C cells were cultured at 37°C in a humidified incubator with 5% CO_2. Culture medium was refreshed every three days throughout the incubation period.

2.2 Bioink Preparation

A collagen–alginate–fibrin (CAF) hydrogel was formulated based on the protocol developed by Montalbano et al. [24]. Fibrinogen (Type I-S from bovine plasma, 65–85% protein;

Sigma-Aldrich, UK) was dissolved in Dulbecco's Phosphate Buffered Saline (DPBS) without calcium and magnesium (Sigma-Aldrich) at a concentration of 37.5 mg/mL and stirred gently at 37°C for 2 hours. Separately, alginic acid sodium salt (Sigma-Aldrich, UK) was dissolved in DPBS at 25 mg/mL and stirred at 40°C for 2 hours. The polymer pre-gel solution was prepared by gradually mixing the fibrinogen and alginate solutions, followed by the addition of Type I collagen (FS22005; 6 mg/mL pepsin-soluble collagen in 0.01 M HCl; Collagen Solutions, UK) in a volumetric ratio of 1:2:8 (collagen: alginate: fibrinogen).

The crosslinking solution was prepared by dissolving 500 U of thrombin (T4648-10KU; Sigma-Aldrich) in 1 mL of DMEM/F12 (Thermo Fisher Scientific), supplemented with 0.1-0.2% calcium chloride ($CaCl_2$; C1016, Sigma-Aldrich).

To create the bio-ink Y201-C cells were resuspended in the crosslinking solution at two cell densities: 10 million cells per mL of crosslinking solution as a "low" density and 50 million cells per mL of crosslinking solution as a "high" density. The ReJI process uses equal volumes of the two starting solutions, and so this results in 5 million and 25 million cells per mL of CAF hydrogel respectively.

2.3 Bioprinting and Cell Seeding

Bioprinting was conducted using a custom-built ReJI bioprinter, as shown in Figure 3. This system features a bespoke printhead designed to create a 55° inclination between two solenoid microvalves (INKX0514950A and B; The Lee Company, Westbrook Center, USA). Each microvalve has a nozzle diameter of 500µm and is actuated via a spike-and-hold driver (The Lee Company, USA). One microvalve is connected to the pre-gel bioink reservoir, while the other is linked to the crosslinker solution reservoir. Pressure to both reservoirs is provided through disc pump systems (The Lee Company, USA).

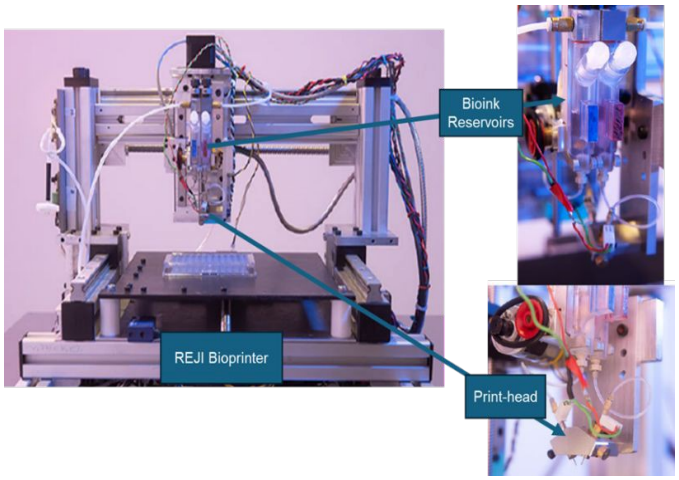

Figure 3 - REJI bioprinter. Main machine structure on left, with close-ups of bio-ink reservoirs and the print head assembly on right.

Printing parameters were controlled a bespoke software system. Droplet ejection was achieved through electrical impulses delivered as rectangular waveforms set to 3.2 V, with a dwell time of 800 µs and an actuation frequency of 100 Hz. Jetting pressure was maintained at 380 mmHg for the crosslinker bioink and 400 mmHg for the pre-gel bioink.

To prevent cell and particle sedimentation during printing an agitation system was used [25]. A 1 mm diameter circular gold-coated disc was placed in both reservoirs and rotated magnetically to provide continuous agitation.

For all cellular studies, CAF hydrogels were bioprinted using a custom script designed for a 96-well plate format, dispensing 67 droplets per well to produce 20 µL of gel per sample at low (CAF-L) and high (CAF-H) cell densities. Chondro-Gide® (Ch-G; Geistlich Pharma AG, Switzerland) patches were used as substrates, punched to a diameter of 6 mm to fit within the wells. CAF gels were bioprinted directly onto Ch-G substrates (Ch-G/CAF) using a bitmap technique (10 × 10 pixels) to enhance integration between the hydrogel and collagen fibres.

For mechanical characterization, CAF gels with and without Ch-G substrates were printed using a bitmap pattern of a circle with a diameter of 25 pixels in two layers, yielding constructs approximately diameter of 8 mm and thickness of 3 mm.

For control samples, cells were manually seeded onto Ch-G patches at densities of 250,000 cells/cm² (Ch-G-L) and 1.25×10^6 cells/cm² (Ch-G-H) to represent low and high cell loading, respectively.

All samples were cultured up to 14 days in a humidified incubator at 37 °C and 5% CO_2 in DMEM/F12 medium supplemented with 10% foetal bovine serum (FBS) and 1% penicillin/streptomycin (P/S).

2.4 Biological Characterisation

2.4.1 Cell viability and survival

A live/dead assay was performed to evaluate the cytotoxicity of the hydrogels using the live/dead Viability/Cytotoxicity Kit (Invitrogen). Samples were first rinsed with DPBS, then incubated in a staining solution containing 4 µM ethidium homodimer-1 and 10 µM calcein in DPBS for 30 minutes at room temperature under light-protected conditions. Following incubation, samples were washed again with DPBS and imaged using an EVOS M5000 inverted confocal microscope (10× magnification) with GFP/RFP fluorescence settings.

2.4.2 Immunofluorescence Staining

Cellular morphology was assessed by staining the cytoskeleton with Alexa Fluor® 555-conjugated phalloidin and the nuclei with 4',6-diamidino-2-phenylindole (DAPI). Following the culture period, samples were rinsed with DPBS and fixed in 4% paraformaldehyde overnight at 4 °C. Subsequently, cells embedded within the hydrogels were permeabilised using 0.1% (v/v) Triton X-100 in DPBS for 40 minutes.

Phalloidin staining solution was prepared at a 1:1000 dilution in DPBS, and samples were incubated for 60 minutes at room temperature under light-protected conditions. After washing with DPBS, samples were stained with DAPI solution (1:300 in DPBS) and incubated for 30 minutes in a light-protected environment at 37 °C. Imaging was performed using a ZEISS LSM 800 confocal microscope at 5× and 10× magnifications.

2.4.3 Scanning Electron Microscopy (SEM) Analysis

Cell morphology in CAF and Ch-G-CAF samples along with Ch-G control samples were analysed using a Tescan Vega LMU (Tescan, Cambridge). Samples were collected on days 7 and 14

View Article Online DOI: 10.1039/D6BM00467A

and rinsed with DPBS. Subsequently, samples were fixed using a 2% glutaraldehyde solution and the samples were stored overnight at 4 °C. Following fixation, all samples were washed with DPBS and dehydrated using 25%, 50%, 75%, and 100% ethanol (EtOH). Samples were kept at 4°C in 100% EtOH until they were subjected to critical point drying using a Baltec Critical Point Dryer (Leica Geosystems Ltd, UK). For imaging, samples were mounted on aluminium stubs and gold coated using a Polaron SEM Coating Unit (Quorum Technologies Ltd, UK). SEM imaging was conducted at an accelerating voltage of 8.0 kV under varying magnifications.

2.4.4 Gene Expression analysis through RT-PCR

Hydrogel samples were digested by incubation in dispase solution overnight at 37 °C. The resulting digested solution was centrifuged, and the cell pellets were stored at −20 °C until further processing. Upon reaching the final time point, total RNA was extracted using the RNeasy Mini Kit (QIAGEN, UK) according to the manufacturer's protocol. RNA concentration and purity were assessed using a NanoDrop spectrophotometer, and all samples were standardized to a concentration of 1 ng/µL.

Complementary DNA (cDNA) synthesis was performed using the High-Capacity cDNA Reverse Transcription Kit (Thermo Fisher Scientific, UK), following the manufacturer's instructions. Quantitative real-time PCR (RT-qPCR) was conducted using TaqMan™ Fast Advanced Master Mix (Thermo Fisher Scientific, UK) and TaqMan gene expression assays targeting Aggrecan (Hs00153936_m1) and Sox9 (Hs00165814_m1). Reactions were run on the QuantStudio™ 7 Real-Time PCR System (Thermo Fisher Scientific, US) using a 40-cycle, three-step amplification protocol.

Gene expression levels were normalized to the housekeeping gene GAPDH (Hs02786624) and quantified using the 2^(-ΔΔCt) method. Expression in control samples was used as the calibrator for relative quantification.

2.4.5 Immunohistochemistry

Samples were immersed in 10% formalin for fixation overnight at 4°C after specific time periods then transferred to histology cassettes and immersed in 70% ethanol. Tissue dehydration was performed using a graded EtOH series (70%, 80%, 95%, and 100%), followed by paraffin embedding. Vertical cross-sections of 4µm thickness were obtained and mounted onto glass slides. Sections were deparaffinized, dewaxed, and rehydrated through descending EtOH concentrations. Non-specific binding was blocked using 20% goat serum. Primary antibody targeting collagen type II (COL II; 1:200 in TBS, PA-26206, Thermo Fisher Scientific) was applied and incubated overnight at 4 °C. The slides were then treated with a polyclonal goat anti-rabbit HRP-conjugated secondary antibody (ab6721, Abcam), and signal development was carried out using the DAB Substrate Kit (Abcam). Counterstaining was performed with Gill's hematoxylin, and slides were mounted using DPX Mountant (Sigma-Aldrich). Imaging was conducted using the EVOS M5000 Imaging System (Invitrogen™, UK) at 10× magnification.

For sulphated glycosaminoglycan (sGAG) detection, sections were counterstained with Alcian Blue and Nuclear Fast Red. Slides were subsequently mounted in DPX and visualized using an Olympus BX51 digital microscope.

2.4.6 Mechanical Characterisation

Compression strength of bioprinted CAF hydrogels, with and without Chondro-Gide®, was assessed using the UniVert Test Device (UV-200–01, CellScale, Canada) equipped with a 10 N load cell. Cylindrical samples (n = 3) were fabricated in 48-well plates, each measuring approximately 8 mm in diameter and 3 mm in height. Compression testing was performed at a crosshead speed of 0.5 mm/min, with loading applied up to 80% strain. Stress–strain curves were generated, and the compressive modulus was calculated from the linear region of the curve between strains of 10 and 15%.

2.4.7 Statistical Analysis

Statistical analysis was conducted using GraphPad Prism 10. Quantitative data were expressed as mean ± standard deviation (SD). Group comparisons were performed using two-way ANOVA followed by Tukey's multiple comparison test. Statistical significance was denoted as follows $p<0.05$ (*), $p<0.01$(**), $p<0.001$ (***) and $p<0.0001$ (****).

3. Results

3.1 Bioprinting Process

The bioprinting process yielded structurally consistent constructs, with representative images of each sample group presented in Figure 4.

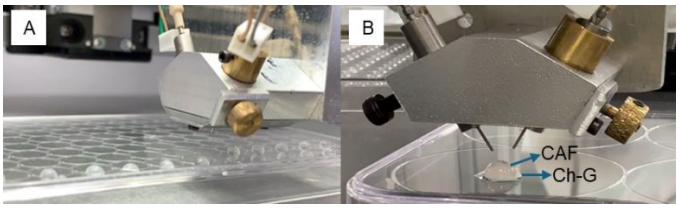

Figure 4 - Representative images of bioprinted samples A) CAF samples on 96 well plate lid and B) Ch-G/CAF sample on 6 well plate lid. Printed on well plate lids for clarity

3.2 Cell Viability

Live/dead assays showed consistently high cell viability across all conditions and time points (Figure 5) for all samples. Similarly, control samples exhibited minimal cell death on both day 1 and day 3, independent of cell density.

3.3 Cell and Culture Morphology

Chondrocyte morphology and cell-cell interactions within CAF gels (Figure 6) showed that from day 7, chondrocyte cells started to stretch out and take on a longer shape. Gels printed with 25 million cells/mL—both with and without the Ch-G substrate—showed stronger cell-to-cell connections. By day 14, these connections became tighter, forming more compact cell structures in the CAF-L, CAF-H and Ch-G/CAF-H cultures.

In the Ch-G/CAF samples, the cells were mostly spread out in a flat, 2D layer because the gel settled on the fibres of the substrate. Ch-G-L and Ch-G-H samples showed similar patterns on day 7 and day 14 for both low and high cell densities, with

View Article Online
DOI: 10.1039/D6BM00467A

cells on interacting with the substrate, with the differences in the two cell densities evident in the cultures.

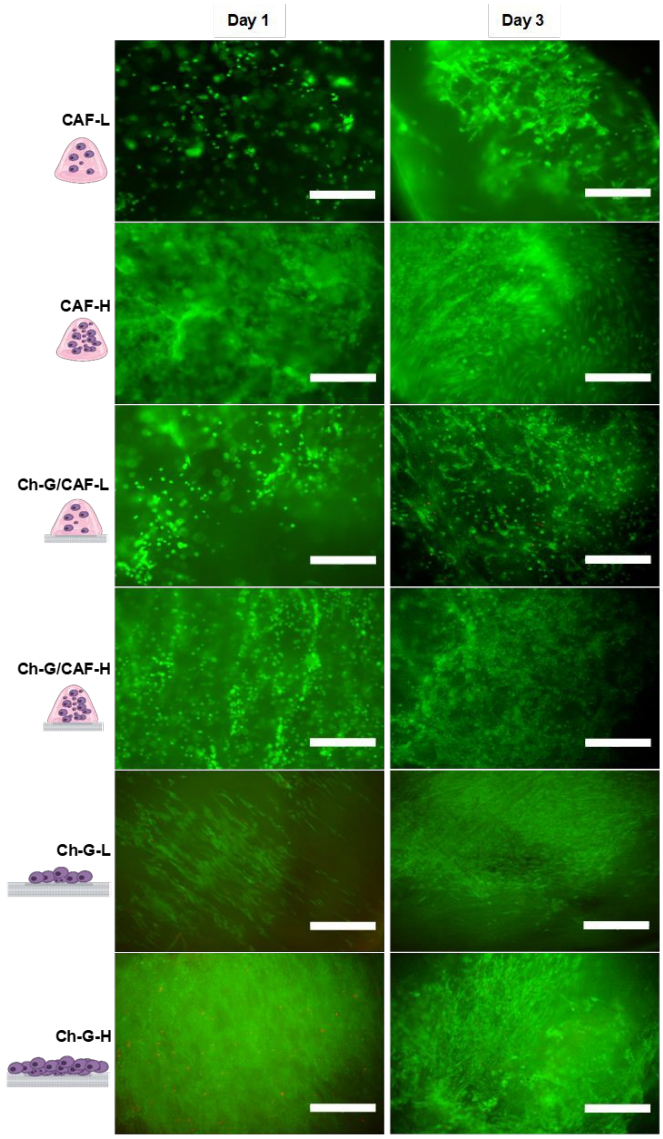

Figure 5 - Live and dead analysis images of CAF hydrogel with and without Ch-G on day 1 and day 3. Scale Bar is 300 µm. Predominance of green fluorescence across all samples qualitatively indicates high cell viability.

3.4 ECM Formation

On day 7, most cells in the CAF gel were embedded within the gel (Figure 7). However, for gels printed on the Ch-G, cells began migrating toward the surface. By day 14, both cell migration and extracellular matrix (ECM) formation were clearly visible in all samples. Printing on Ch-G appeared to speed up this surface migration and supported earlier ECM deposition. These samples showed strong cell attachment and growth along the fibres, forming a monolayer-like structure.

3.5 Chondrogenic Gene Expression

SOX9 expression (Figure 8) was lowest in samples without Ch-G, and notably higher in Ch-G-H on day 1 ($p<0.05$), but then broadly showed a similar level of expression at day 14 as seen at day 1. ACAN expression showed a sharp and consistent increase ($p<0.01$) across all sample groups from day 1 to day 14. Whilst no significant differences were observed in ACAN expression between manual seeding and printing of the cells on a substrate, a significant difference was noted between low and high cell densities in both Ch-G and Ch-G/CAF samples.

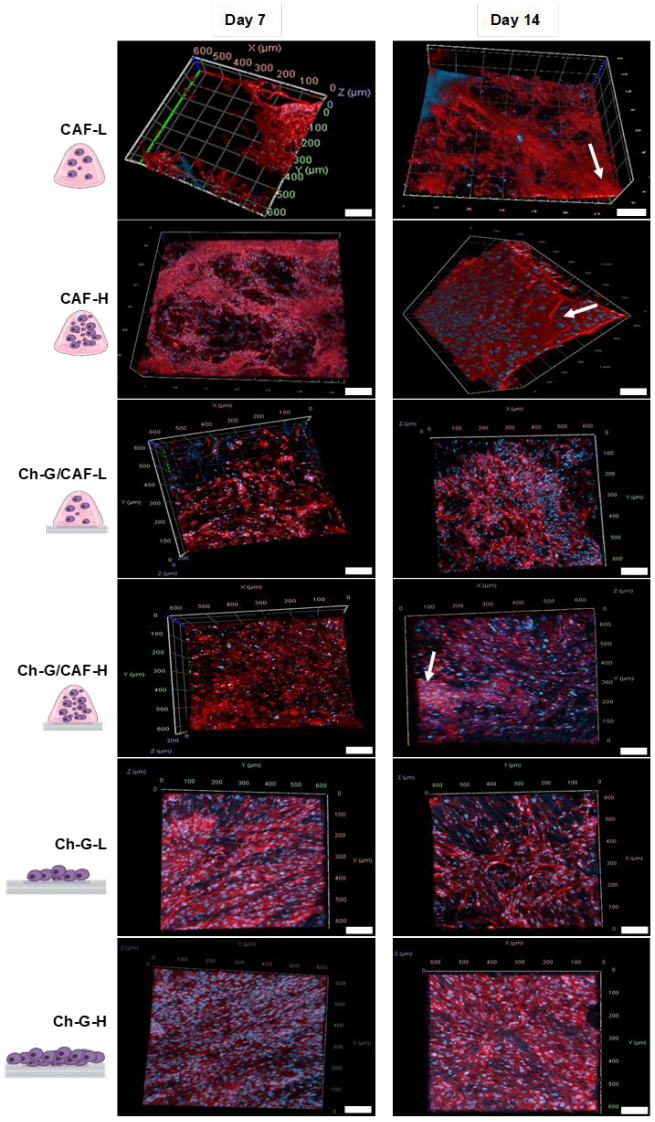

Figure 6 - Confocal images of chondrocyte cells in all groups- CAF, Ch-G/CAF and Ch-G on days 7 and 14. Images are 600 x 600 µm, scale bar is 100 µm Blue: nuclei, red: F-actin cytoskeleton. Chondrocytes show an elongated morphology, and higher cell densities show greater tendency to produce dense cellular aggregates within the cultures. White arrows highlight compact cell structures.

3.6 Protein Production

Among all groups, the Ch-G/CAF-H samples exhibited the highest Collagen II expression (Figure 9), indicated by intense brown staining. In the control samples, CH-G-H showed greater Collagen II production than CH-G-L. Similarly, GAG expression was markedly higher in Ch-G/CAF-H samples compared to all other conditions. This suggests that bioprinting high cell density CAF gels onto Chondro-Gide® substrates significantly enhances the secretion of both Collagen II and sGAG, supporting improved matrix formation and chondrogenic activity.

View Article Online
DOI: 10.1039/D6BM00467A

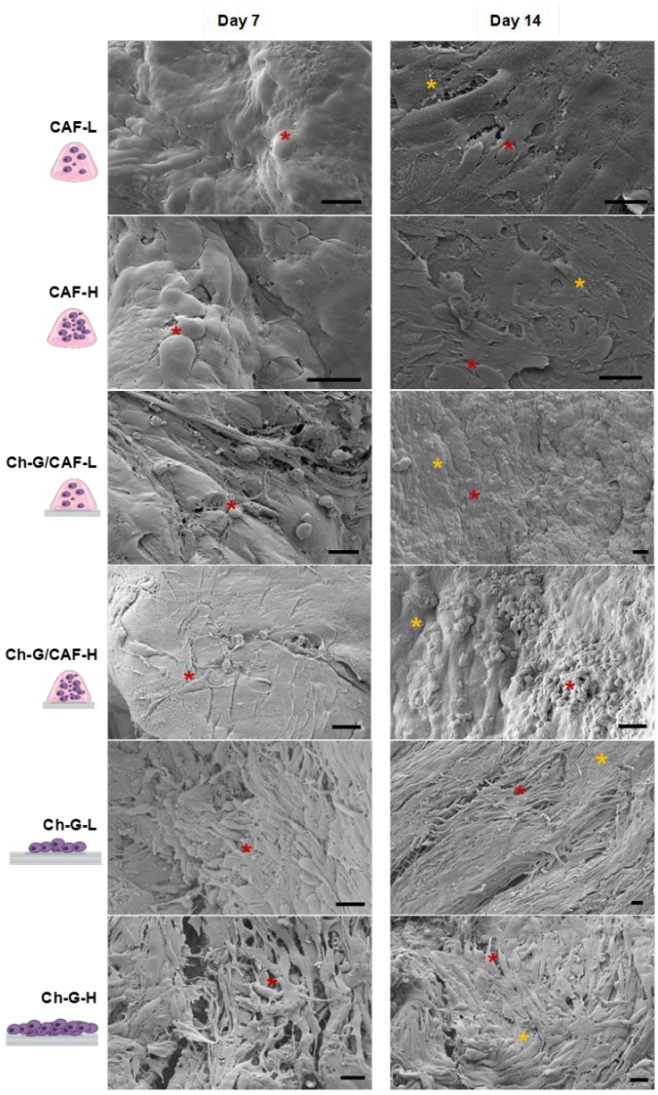

Figure 7 - Morphology of all sample groups – CAF, Ch-G/CAF and Ch-G after incubating for 7 and 14 days by SEM, scale bar: 25 µm. Red stars indicate chondrocytes, while yellow stars highlight ECM deposition. Cultures show cell migration and ECM production.

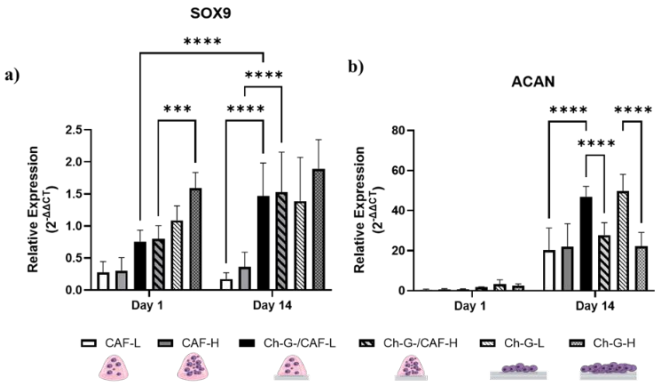

Figure 8 - Gene Expression of Y201-C cells in CAF, CH-G and Ch-G/CAF samples after incubating for 1 and 14 days. a) SOX9, b) ACAN. Expression of SOX9 similar at days 1 and 14 for all samples, but higher in all Ch-G samples, whilst ACAN expression is higher across all cultures at day 14, with expression of ACAN in low cell density Ch-G samples the highest at day 14. Statistical significance was indicated as follows: p<0.05 (*), p<0.01(**), p<0.001 (***) and p<0.0001 (****)

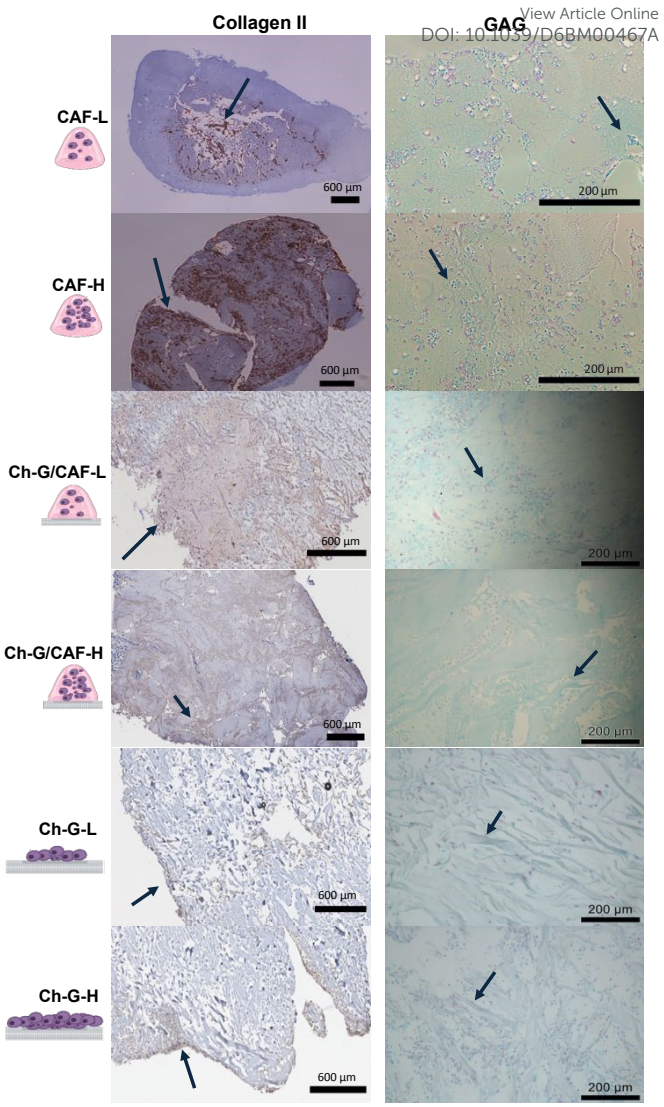

Figure 9 - Immunohistochemical staining of all sample groups on Day 14: Collagen II (Left) and sGAG proteins (Right). Brown staining indicates Collagen II deposition; blue staining indicates sGAG protein deposition.

3.7 Compression Modulus and Volume Changes

Over the 14-day period, a significant increase in compressive modulus was observed in all groups ($p<0.05$) except for the acellular gels ($p>0.05$), as shown in Figure 10. Although there was no significant difference on day 1 in CAF sample group, as the matrix formed a notable difference is shown on day 14 samples ($p<0.01$), with a similar trend was observed in CH-G/CAF samples group. All samples were significantly different to each other except CH-G/CAF and Ch-G/CAF-L on day 1 ($p>0.05$). Notably, on day 14, the Ch-G/CAF samples exhibited significantly higher compressive modulus values, irrespective of cellular density as there was no significant difference between low and high cell densities ($p>0.05$).

There was no significant difference in volume in most of the groups from D1 to D14, except for the Ch-G/CAF-L samples (Figure 11). Overall, gels incorporating Ch-G exhibited generally higher volumes compared to their CAF-only samples at both day

View Article Online
DOI: 10.1039/D6BM00467A

1 and day 14, arising from the inclusion of the membrane volume, but the main observation is that for all samples the volume was essentially maintained across the culture period.

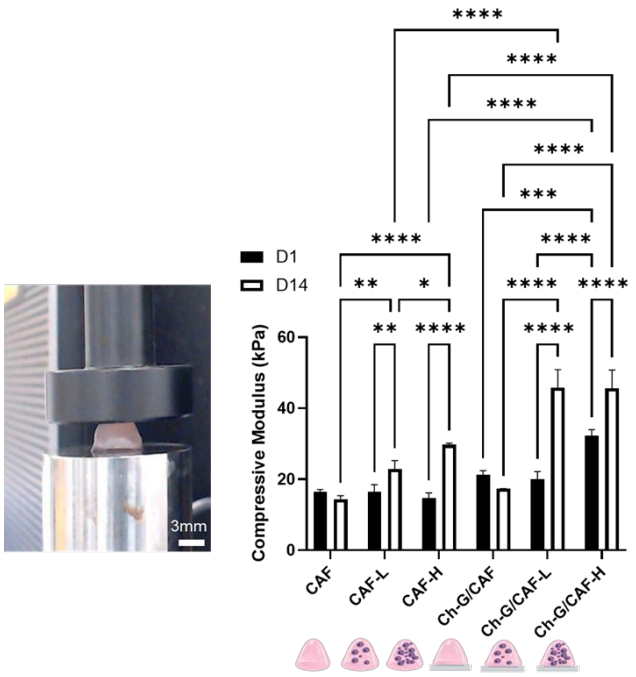

Figure 10 - Left: Representative compression test image and Right: Compressive modulus of CAF and Ch-G/CAF samples on day 1 and day 14. Statistical significance was indicated as p<0.05 (*), p<0.01(**), p<0.001 (***) and p<0.0001 (****).

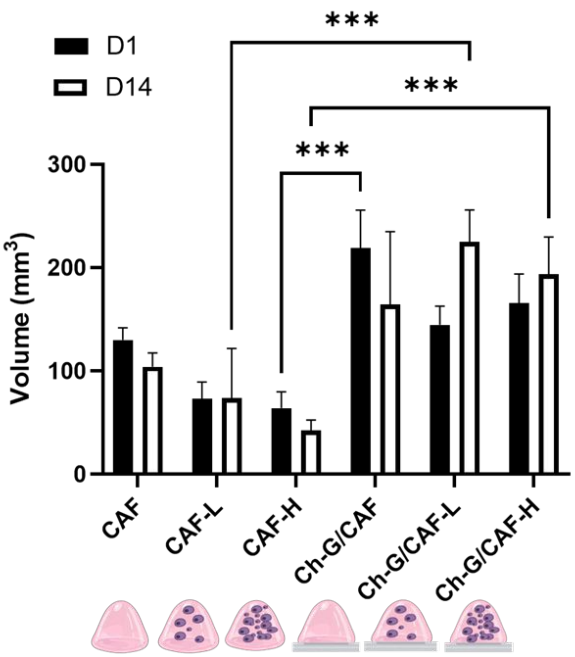

Figure 11 - Volumetric analysis of gel constructs on day 1 and day 14. Statistical significance was indicated as follows: p<0.05 (*), p<0.01(**) and p<0.001 (***).

4. Discussion

4.1 Cell Viability and Function

Live/dead assays demonstrated high cell viability across all constructs, in line with previous studies reporting minimal cytotoxicity across various cell lines [16, 18, 19]. From day 1 to day 3, an increase in the amount of cells could be observed qualitatively.

Both ICC and morphology imaging demonstrated good cellular alignment and networking from day 7 to day 14, particularly in high-density constructs. The enhanced surface migration and alignment along collagen fibres in the Ch-G/CAF samples suggests that the fibrous membrane supports cell attachment and also facilitates directional migration and organization, which are critical for effective tissue regeneration, in line with earlier observations [18]. The cell filled CAF hydrogels support this process by providing a reservoir of chondrocytes, fixed in space, which can gradually migrate to colonise the structure. By day 14, a thick ECM-like layer [26] was observed across all samples, with the highest deposition seen in the Ch-G/CAF-H group.

A key limitation in ACI is the de-differentiation of chondrocytes during in vitro expansion, often accompanied by altered extracellular matrix regulation [27, 28]. To overcome this, it is essential to promote chondrogenesis and support the development of a cartilage-specific matrix rather than a fibroblastic matrix. In our study, a key ECM component gene, ACAN, showed a significant upregulation indicating active-matrix synthesis. Similarly, SOX9, the master regulator chondrogenesis gene, was elevated in the Ch-G group, suggesting that the Ch-G membrane promotes chondrogenesis [29].

4.2 Matrix Production

For any ACI type procedure the key outcome is cartilage repair, and for this reason we have focussed on matrix production as the factor in assessing the combination of ReJI bioprinting and Chondro-Gide® as a new variant of the MACI process. It's clear that within the context of this in vitro assessment that the combined approach has led to greater matrix deposition than either (i) printed hydrogels alone, or (ii) cells suspended in media seeded onto Chondro-Gide®.

As SOX9 and ACAN are key regulators of cartilage matrix formation promoting the synthesis of collagen type II and glycosaminoglycans (GAGs) and it is essential to assess not only their gene expression but also the actual deposition of these matrix components within the extracellular environment [28-30]. Evaluating the presence of these proteins and proteoglycans in the matrix provides critical insight for chondrogenic differentiation and the effectiveness of ACI treatment. Collagen II and aggrecan are the most abundant proteins in cartilage and together they play an important role in cartilage regeneration [31]. Immunohistochemistry showed intense Collagen II and GAG staining in Ch-G/CAF-H samples. These results highlight the combined influence of high cell density and substrate integration in enhancing chondrogenic activity and matrix deposition, consistent with prior studies demonstrating

improved ECM formation in co-culture and high-density environments [29, 32, 33].

The stability of construct dimensions over time is essential for clinical translation, as it ensures consistent defect coverage and mechanical support during regeneration. Compression testing revealed a significant increase in Young's modulus from day 1 to day 14 in all cellular constructs, with Ch-G/CAF samples exhibiting the highest stiffness. This mechanical enhancement correlates with ECM accumulation and cellular remodelling, suggesting that the bioprinted constructs are progressing toward cartilage-like mechanical behaviour. Although the modulus remains below native cartilage levels (0.3–0.8 MPa) [34-36], the observed trend supports the potential for further maturation with extended culture. These findings are consistent with previous reports that ECM deposition contributes to increased gel stiffness, particularly in co-culture and high-density conditions [37]. Volumetric analysis showed that Ch-G/CAF constructs maintained higher volumes compared to CAF-only gels, indicating better structural integrity and possibly enhanced matrix retention. That the Ch-G/CAF-L was the only group to show an increase in volume over the culture period was interesting. Although this was not statistically significant it's possible that this comes from cell proliferation within the culture. The CAF-L gel group would not have the benefit of the Chondro-gide®, whilst the higher cell density in the Ch-G/CAF-H group would result in contact inhibition, reducing proliferation.

4.3 MACI with In-clinic Bioprinting

We consider this study to have shown that combining ReJI bioprinting in clinic with a Chondro-Gide® membrane could offer an enhanced approach to MACI. The overall process would still require harvesting of cartilage, followed by isolation and expansion of the chondrocytes, but the chondrocytes would then be printed in clinic onto the Chondro-Gide® prior to implantation. The potential additional clinical value arising from the bioprinting process would be that this would allow cells to be distributed as required throughout the volume of the defect: an even distribution if required, or concentrating the chondrocytes close to the Chondro-Gide® or towards the osteochondral interface. Encapsulation of the cells could also minimise cell loss during implantation. This could address recognised issues with both cell loss and uneven distribution at the defect site [8, 9], potentially leading to a quicker repair at the defect site, although further studies will be required to demonstrate this.

Looking further forward, some researchers are evaluating extending ACI type procedures to also deliver mesenchymal stem cells (MSCs) alongside the chondrocytes [38-40], to give an enhanced therapeutic effect. ACI-MSC procedures could benefit from bioprinting through allowing scope for the types of co-culture used (mixed, stratified, or zonal, or a combination of these) and for the gradient distribution of both types of cells through the defect volume.

5. Conclusions

View Article Online
DOI: 10.1039/D6BM00467A

The integration of high-density cell-laden CAF hydrogels with Chondro-Gide® substrates via ReJI bioprinting offers a promising strategy for next-generation MACI. This approach enhances cell viability, proliferation, ECM production, and mechanical performance, addressing key limitations of traditional ACI techniques. Future work will develop the approach towards in vivo studies.

6. Author contributions

Conceptualization: Dalgarno; Data Curation: Ozdemir Steedman; Formal Analysis: Ozdemir Steedman; Funding Acquisition: Dalgarno; Investigation: Ozdemir Steedman; Methodology: Ozdemir Steedman, Ferreira, Melo and Dalgarno; Project Administration: Dalgarno; Resources: Ferreira, Melo and Dalgarno; Supervision: Ferreira, Melo and Dalgarno; Writing-original draft: Ozdemir Steedman and Dalgarno; Writing-review & editing: Ozdemir Steedman, Ferreira, Melo and Dalgarno.

7. Conflicts of interest

Newcastle University have established a spin-out company, Jetbio, to exploit the reactive jet impingement process. Dalgarno, Ferreira and Melo are all shareholders in Jetbio.

8. Data availability

The raw data that underpins this study are openly available in the Newcastle University Research Repository at doi: 10.25405/data.ncl.30819365.

9. Acknowledgements

This project has received funding from the (i) UK EPSRC through award EP/V013092/1, (ii) Arthritis UK (formerly Versus Arthritis) through the Tissue Engineering and Regenerative Therapies Centre Versus Arthritis (Award 21156), and (iii) UK National Centre for the Replacement, Refinement and Reduction of Animals in Research (NC3Rs) through award APP46911. We are also grateful to Prof. Paul Genever (University of York) for provision of the Y201 cell line and to Geistlich Pharma AG for providing the Chondro-Gide® membranes. Figures 1 and 2 were developed using BioRender.

10. Notes and references

1. Courties A, Kouki I, Soliman N, et al. Osteoarthritis year in review 2024: Epidemiology and therapy. *Osteoarthritis and Cartilage* 2024; 32: 1397-1404.
2. Ossendorff R, Grede L, Scheidt S, et al. Comparison of minced cartilage implantation with autologous chondrocyte transplantation in an in vitro inflammation model. *Cells* 2024; 13: 546.
3. Zhou Y, Qin R, Chen T, et al. 3D bioprinting modified autologous matrix-induced chondrogenesis (AMIC) technique for repair of cartilage defects. *Materials & Design* 2021; 203: 109621.

4. Davies RL and Kuiper NJ. Regenerative medicine: a review of the evolution of autologous chondrocyte implantation (ACI) therapy. *Bioengineering* 2019; 6: 22.
5. Hulme CH, Perry J, McCarthy HS, et al. Cell therapy for cartilage repair. *Emerging topics in life sciences* 2021; 5: 575-589.
6. Niemeyer P and Angele P. Autologous chondrocyte implantation (ACI) for cartilage defects of the knee using Novocart 3D and Novocart inject. *Operative Techniques in Sports Medicine* 2022; 30: 150959.
7. Vonk LA, Roël G, Hernigou J, et al. Role of matrix-associated autologous chondrocyte implantation with spheroids in the treatment of large chondral defects in the knee: a systematic review. *International Journal of Molecular Sciences* 2021; 22: 7149.
8. Jiang YZ, Zhang SF, Qi YY, et al. Cell transplantation for articular cartilage defects: principles of past, present, and future practice. *Cell transplantation* 2011; 20: 593-607.
9. Karami P, Laurent A, Philippe V, et al. Cartilage repair: Promise of adhesive orthopedic hydrogels. *International journal of molecular sciences* 2024; 25: 9984.
10. Tierney L, Kuiper JH, Roberts S, et al. Lower cell number, lateral defect location and milder grade are associated with improved autologous chondrocyte implantation outcome. *Knee Surgery, Sports Traumatology, Arthroscopy* 2025; 33: 1308-1320.
11. Guillén-García P, Guillén-Vicente I, Rodríguez-Iñigo E, et al. Cartilage defect treatment using high-density autologous chondrocyte implantation (HD-ACI). *Bioengineering* 2023; 10: 1083.
12. Foldager CB, Gomoll AH, Lind M, et al. Cell seeding densities in autologous chondrocyte implantation techniques for cartilage repair. *Cartilage* 2012; 3: 108-117.
13. Jacob GT, Passamai VE, Katz S, et al. Hydrogels for extrusion-based bioprinting: General considerations. *Bioprinting* 2022; 27: e00212.
14. Dell AC, Wagner G, Own J, et al. 3D bioprinting using hydrogels: cell inks and tissue engineering applications. *Pharmaceutics* 2022; 14: 2596.
15. Ning L and Chen X. A brief review of extrusion-based tissue scaffold bio-printing. *Biotechnology journal* 2017; 12: 1600671.
16. da Conceicao Ribeiro R, Pal D, Ferreira AM, et al. Reactive jet impingement bioprinting of high cell density gels for bone microtissue fabrication. *Biofabrication* 2018; 11: 015014.
17. Ozdemir Steedman F, Ruiz Gutierrez E, Tzivelekis C, et al. Effect of bio-ink physical properties on droplet volume in the reactive jet impingement 3D bioprinting system. *Journal of the Mechanical Behavior of Biomedical Materials* 2026: 107471.
18. Kotlarz M, Ferreira AM, Gentile P, et al. Droplet-based bioprinting enables the fabrication of cell–hydrogel–microfibre composite tissue precursors. *Bio-Design and Manufacturing* 2022; 5: 512-528.
19. Kotlarz M, Melo P, Ferreira AM, et al. Cell seeding via bioprinted hydrogels supports cell migration into porous apatite-wollastonite bioceramic scaffolds for bone tissue engineering. *Biomaterials Advances* 2023; 153: 213532.
20. Bowes A, Collins A, Oakley F, et al. Bioprinted high-cell-density laminar scaffolds stimulate extracellular matrix production in osteochondral co-cultures. *International Journal of Molecular Sciences* 2024; 25: 11131.
21. James S, Fox J, Afsari F, et al. Multiparameter analysis of human bone marrow stromal cells identifies distinct immunomodulatory and differentiation-competent subtypes. *Stem cell reports* 2015; 4: 1004-1015.
22. Scalzone A, Cerqueni G, Wang XN, et al. A cytokine-induced spheroid-based in vitro model for studying osteoarthritis pathogenesis. *Frontiers in Bioengineering and Biotechnology* 2023; 11: 1167623.
23. Scalzone A, Wang XN, Dalgarno K, et al. A chondrosphere-based scaffold free approach to manufacture an in vitro articular cartilage model. *Tissue Engineering Part A* 2022; 28: 84-93.
24. Montalbano G, Toumpaniari S, Popov A, et al. Synthesis of bioinspired collagen/alginate/fibrin based hydrogels for soft tissue engineering. *Materials science and engineering: C* 2018; 91: 236-246.
25. Dudman JP, Ferreira AM, Gentile P, et al. Reliable inkjet printing of chondrocytes and MSCs using reservoir agitation. *Biofabrication* 2020; 12: 045024.
26. Barreto-Henriksson H, Llorente M, Larsson A, et al. Determination of mechanical and rheological properties of a cell-loaded peptide gel during ECM production. *International Journal of Pharmaceutics* 2019; 563: 437-444.
27. Wang M, Iwahashi T, Kasuya T, et al. Effects of a Novel Mammalian-Derived Collagen Matrix on Human Articular Cartilage-Derived Chondrocytes from Osteoarthritis Patients. *International Journal of Molecular Sciences* 2025; 26: 7826.
28. Takahashi T, Brown WE, Trinh CT, et al. Formation of functionally robust human neocartilage from multiple donors using highly expanded costochondral cells. *Biofabrication* 2025; 17: 035020.
29. Lu H, Hoshiba T, Kawazoe N, et al. Cultured cell-derived extracellular matrix scaffolds for tissue engineering. *Biomaterials* 2011; 32: 9658-9666.
30. Miao Z, Lu Z, Wu H, et al. Collagen, agarose, alginate, and Matrigel hydrogels as cell substrates for culture of chondrocytes in vitro: A comparative study. *Journal of cellular biochemistry* 2018; 119: 7924-7933.
31. Roughley PJ and Mort JS. The role of aggrecan in normal and osteoarthritic cartilage. *Journal of experimental orthopaedics* 2014; 1: 1-11.
32. Richardson SM, Hughes N, Hunt JA, et al. Human mesenchymal stem cell differentiation to NP-like cells in chitosan–glycerophosphate hydrogels. *Biomaterials* 2008; 29: 85-93.
33. Eschen C, Kaps C, Widuchowski W, et al. Clinical outcome is significantly better with spheroid-based autologous chondrocyte implantation manufactured with more stringent cell culture criteria. *Osteoarthritis and Cartilage Open* 2020; 2: 100033.
34. Korhonen R, Laasanen M, Töyräs J, et al. Comparison of the equilibrium response of articular cartilage in unconfined compression, confined compression and indentation. *Journal of biomechanics* 2002; 35: 903-909.
35. Camarero-Espinosa S, Tomasina C, Calore A, et al. Additive manufactured, highly resilient, elastic, and biodegradable poly (ester) urethane scaffolds with chondroinductive properties for cartilage tissue engineering. *Materials Today Bio* 2020; 6: 100051.
36. Petitjean N, Canadas P, Royer P, et al. Cartilage biomechanics: From the basic facts to the challenges of tissue engineering. *Journal of Biomedical Materials Research Part A* 2023; 111: 1067-1089.
37. Frantz C, Stewart K and Weaver V. The extracellular matrix at a glance. J Cell Sci123: 4195–4200. 2010.
38. Wang J, Wright KT, Perry J, et al. Combined autologous chondrocyte and bone marrow mesenchymal stromal cell implantation in the knee: An 8-year follow up of two first-in-man cases. *Cell Transplantation* 2019; 28: 924-931.
39. De Bari C and Roelofs AJ. Stem cell-based therapeutic strategies for cartilage defects and osteoarthritis. *Current opinion in pharmacology* 2018; 40: 74-80.

View Article Online
DOI: 10.1039/D6BM00467A

40. Epanomeritakis IE, Lee E, Lu V, et al. The use of autologous chondrocyte and mesenchymal stem cell implants for the treatment of focal chondral defects in human knee joints—a systematic review and meta-analysis. *International Journal of Molecular Sciences* 2022; 23: 4065.

View Article Online
DOI: 10.1039/D6BM00467A

Bioprinting Chondrocyte Hydrogel Cultures onto Fibre Membranes for Cartilage Defect Repair

Fatma Ozdemir Steedman, Ana Marina Ferreira, Priscila Melo and Kenneth Dalgarno*

* Corresponding Author, kenny.dalgarno@newcastle.ac.uk

The raw data that underpins this study are openly available in the Newcastle University Research Repository at doi: 10.25405/data.ncl.30819365.